

## Parameter Sensitivity in Microsphere Impact and Capture

*R. M. Brach, X. Li, and P. F. Dunn*

DEPARTMENT OF AEROSPACE AND MECHANICAL ENGINEERING,  
UNIVERSITY OF NOTRE DAME, NOTRE DAME, IN 46556

---

**ABSTRACT.** In the presence of adhesion and under certain conditions a microsphere will be captured during a low speed impact with a substrate. The sensitivity of the capture velocity (the largest initial normal velocity at which capture occurs) to five physical factors is analyzed in this paper. The factors are the Hertzian stiffness, Dupré surface energy, the microsphere radius, a damping coefficient associated with adhesion dissipation, and one associated with material dissipation. The sensitivity is determined by examining the effects of the factors on the capture velocity using a two-level, fractional factorial design layout. Capture velocities are determined using analytical models. Results indicate that the Dupré surface energy and the microsphere radius by far play the greatest role in the capture process. The Hertzian stiffness and the dissipation coefficient associated with adhesion affect capture to a lesser extent; an interaction of the surface energy and the adhesion energy dissipation can also play a small role.

---

### INTRODUCTION

When microparticles (particles in the nominal size range from about 1  $\mu\text{m}$  to 100  $\mu\text{m}$ ) with an initial normal velocity move into contact with other particles or a surface (substrate), they are subject to a variety of special contact forces. These include electrostatic, capillary, contact potential, gravitational, and van der Waals forces. Adhesion, primarily the van der Waals force, is the result of molecular attraction across the contact interface. It is the force considered in this paper. Although a great deal is known about microparticle contact forces, many questions still remain. The van der Waals force is known to interact with and be influenced by body deformations (Israe-

lachvili 1985). From the static, particle-surface interaction studies of Derjaguin et al. (DMT; 1975), Johnson et al. (JKR; 1971) and others, it is known that the force acts as an attraction force distributed in proximity to the periphery of and in equilibrium with a compressive force distributed within the contact area. The distributed compressive force usually is modeled using Hertzian mechanics. Johnson and Pollock (1994) indicate that adhesion is irreversible and bidirectional with considerably more work needed to separate a particle from a surface than the work of attraction. Experiments by Horn et al. (1987) provide experimental confirmation and illustrations of this behavior. Among behavior not well known

is the nature of how tangential contact forces, namely the friction, combine with van der Waals force and whether or not models such as the Amontons–Coulomb law are appropriate. Also not well known is the dynamic behavior of the adhesion process, particularly energy dissipation associated with these forces during impact. Other unknowns include a lack of knowledge of material properties of microparticles as influenced by size effects and by high strain rates. Finally, direct observation and measurements of displacements, forces, stresses, and deformations during impact currently are practically impossible.

It is well known that microparticles can attach to other particles and/or surfaces during low speed impact, a process referred to as *capture*. Unfortunately, the conditions of dynamic attachment cannot be measured directly because most experimental measurements are designed to measure and compare approach and rebound kinematics. If rebound doesn't occur, most instruments and measurement schemes are ineffective. So attachment conditions often are extrapolated from measurements at initial velocities as near as possible to capture. Although difficult experimentally, modeling of capture can be done relatively easily with the use of analytical models of the impact process. In this paper, two such analytical models and a curve fitting procedure to extrapolate to capture conditions (see Brach and Dunn 1995) are used to relate capture to the physical parameters of the impact and adhesion processes. The analytical models have been validated experimentally and some values of the models' parameters are based on experimental data. Using these models together with methods from the design of experiments (DOE), this paper examines the sensitivity of the capture process to the impact and adhesion process parameters.

A few comments are made here for the benefit of readers unfamiliar with the DOE. An analogy can be drawn to the *method of least squares* and *statistical regression analysis*. The method of least squares can be used as a curve fitting technique without reference to any statistical properties of the points forming the curve. On the other hand, with knowledge of the statistical properties of the distribution of the points, statistical tests can be applied and inferences drawn using methods of regression analysis. Likewise, DOE can be viewed simply as a scheme or approach for systematically and efficiently laying out a set of experiments, in this paper, "computer experiments." It is a linear, orthogonal, multidimensional model of the response contrasts that reveals the relative importance of the parameters that control the measured response, here, the capture velocity computed from analytical models. On the other hand, if the statistical properties of the input data are taken into account, tests of the significance and inferences can be drawn. This is not done in this paper; no hypothesis testing is done and no statistical inferences are made. Conclusions from the results of the application of the DOE are made only about the relative importance of the various process factors.

Briefly, the procedure followed is first to identify the most important physical quantities associated with microparticle impact process. These (material stiffness, surface energy, microsphere radius, and two dissipation constants) are treated as *factors* that control the *response* (capture velocity). Because of the availability of experimental data (Li et al. 1999 and Dunn et al. 1995), the factor values correspond to stainless steel microspheres and a silicon surface and their ranges are chosen to represent realistic variations. According to the DOE the response is calculated for combinations

of high and low values of the factors based on a fractional factorial layout. The results are then analyzed using the linear, orthogonal DOE response-factor relationships to assess the relative importance of the factors on controlling the response. This is done for high and low levels of the factors chosen on the basis of two criteria. The first attempts to estimate *realistic* variations as encountered in experimental measurements and theoretical determination of the nominal values of the factors. The other is a *uniform* percentage variation about the nominal values.

## IMPACT MODELS

Despite an incomplete knowledge of the impact and capture process, two fairly effective engineering models of the impact process have been developed by Brach and Dunn (1995). The first is a *simulation* model. To the authors' knowledge, this is the only model of microsphere impact that can predict capture, that specifically introduces dissipation due to the adhesion process (as opposed to attributing all energy loss to plastic deformation in the materials), and that explicitly contains the factors listed above. This model uses a line attraction force,  $2\pi af_0$ , distributed around the periphery of a circular contact region to represent the van der Waals force, where  $a$  is the dynamic contact radius and  $f_0$  is the adhesion force per unit length. Hertzian mechanics and velocity dependent material and adhesion dissipation are combined to develop a hysteresis-type force throughout an impact cycle. All of the microparticle and process parameters are calculated from known physical processes except the dynamic dissipation constants  $\zeta_A$  and  $\zeta_H$ . These are determined by matching the simulation to experimental results. Once determined, these are held fixed and the simulation predicts rebound and capture for all

other values of the physical process parameters. The model itself is a system of ordinary differential equations of motion of a microsphere integrated numerically to produce displacement, velocities, and forces.

The second model developed by Brach and Dunn (1995) is based on rigid body impact theory and is referred to as a *rigid body impact* model. This is an algebraic model that uses coefficients to represent the material and adhesion process behavior. The coefficients are the coefficient of restitution,  $R$ , defined in the absence of adhesion, an overall coefficient of restitution,  $e$ , in the presence of adhesion, an adhesion coefficient,  $\rho$ , and a tangential impulse ratio coefficient.<sup>1</sup> The coefficients and the capture velocity are dependent on the system parameters and the initial normal velocity. The dependence of the overall coefficient of restitution and the capture velocity,  $v_c$ , on the initial velocity is represented by a set of algebraic equations whose constants are determined by fitting impact response data. These *fitted equations* are based on these coefficients and are used with the rigid body model to predict microsphere impact and capture velocity.

In this paper, the two models and the fitted equations are combined through the following sequence to calculate the capture velocity for the chosen factor values for the DOE sensitivity study:

1. experimental data is used to determine the dissipation coefficients  $\zeta_A$  and  $\zeta_H$  of the simulation model,
2. the simulation model is used to determine the impact behavior over a wide range of initial conditions,
3. the simulation results are used to determine the constants of the fitted equa-

---

<sup>1</sup>The impulse ratio coefficient is not used here because only normal (not oblique) collisions are considered.

tions of the rigid body model, including the capture velocity.

### CALCULATION OF FACTOR LEVELS AND CAPTURE VELOCITIES

Five basic factors are selected from the process of impact with adhesion. These five (which are dependent on the other physical parameters listed in the Nomenclature) are the microsphere radius,  $r$ , the Hertzian stiffness,  $K$ , the Dupré surface energy,  $w_A$ , the damping constant,  $\zeta_A$ , associated with adhesion energy dissipation, and the damping constant,  $\zeta_H$ , associated with material energy dissipation. An analysis using the DOE approach (see Guttman et al. 1982) requires that each factor be assigned low and high values ( $- / +$ ). The capture velocity is calculated from simulations of the impact process for the low and high factor combinations. Finally, the significance of each factor is estimated and all are compared.

Although the DOE itself is not necessarily a statistical model, input quantities (factors) have a statistical basis and statistics plays a role in interpreting the output. Values of the factors now are computed that generally correspond to microsphere and substrate materials used in experiments by Li et al. (1999). It is assumed that these factors are random variables and possess a statistical distribution that can be approximated as Gaussian with mean  $\mu$  and variance  $\sigma^2$ . Each nominal value is treated as the mean, and variations are estimated and used to approximate the variance. Variations of some factors (such as the distribution of particle radii) are representative of an experimentally sampled statistical distribution. In other cases (such as the Hertzian stiffness), the range of factor values represents uncertainty in the physical properties of the materials. Two sets of low and high values of the factors are determined. The

first is referred to as *realistic* variations and corresponds to  $\pm 1\sigma$  (one standard deviation) of the assumed distributions of the factors. The second is a set of *uniform* variations of  $\pm 5\%$  of the nominal values. Each of these two sets then is subjected to a sensitivity analysis based on the DOE. A detailed description of the determination of what are referred to as the *realistic variations* is now given.

#### Hertzian Stiffness, $K$

The Hertzian stiffness is determined from the following equation:

$$K = \frac{4}{3\pi(k_1 + k_2)}, \quad (1)$$

where  $k_i = (1 - \nu_i^2)/(\pi E_i)$ . For the experimental results, the microspheres (material  $i = 1$ ) are made of type 316 stainless steel. Young's modulus varies from 190 to 210 GPa and Poisson's ratio from 0.27 to 0.30 (Gere and Timoshenko 1990). The substrate surface (material  $i = 2$ ) is cut from a silicon wafer. Its Young's modulus varies with crystal orientation and typically can range from 130 to 169 GPa and Poisson's ratio ranges from 0.20 to 0.36 (Wortman and Evans 1965). These variations of physical constants and Equation 1 produce an estimated Gaussian distribution  $N(\mu_K, \sigma_K^2) = N(124.6, 28.1)$ , and a variation of one standard deviation is  $\pm \sigma_K = \pm 5.3$  GPa. So the experimental low and high values of  $K$  are 119.4 and 130.0 and the uniform low and the values of  $K$  are 118.5 and 130.9 GPa.

#### The Dupré Surface Energy, $w_A$

The next factor to be estimated is the Dupré surface energy. In the simulation, the adhesion force,  $F_{adh}$ , is modeled as a ring force

around the contact periphery

$$F_{adh} = 2\pi af_0, \quad (2)$$

where  $f_0$  is the adhesion force per unit length and  $a$  is the instantaneous contact radius. From the equation of motion along the normal direction (Brach and Dunn 1995), at the equilibrium state, the adhesion force must balance the Hertzian force, so

$$\sqrt{r} Kn^{3/2} = 2\pi af_0, \quad (3)$$

where  $n$  is the normal displacement of the mass center due to elastic deformation. According to Hertzian theory, the displacement is related to the contact radius such that  $n = a^2/r$ . Substituting this relation into Equation 3 gives

$$f_0 = Ka_{eq}^2/2\pi r. \quad (4)$$

From the derivation of JKR theory (Johnson et al. 1971), the equilibrium contact radius,  $a_{eq}$ , is

$$a_{eq}^3 = 6w_A\pi r^2/K, \quad (5)$$

in which  $w_A$  is the Dupré surface energy. Therefore,  $f_0$  becomes

$$f_0 = (6w_A)^{2/3}(Kr/8\pi)^{1/3}. \quad (6)$$

Theoretically, the adhesion force per unit length could easily be determined from Equation 6 using the materials' surface energy. Unfortunately, the Dupré surface energy is available for very few practical materials. However, according to Lee (1991),

$$w_A = F_1 + F_2 - F_{1,2}, \quad (7)$$

where  $F_1$  and  $F_2$  are the surface free energies of body 1 and body 2, respectively, and  $F_{1,2}$  is the interfacial free energies. In practice,  $\gamma_1$  and  $\gamma_2$ , the surface tensions of the two bodies and  $\gamma_{1,2}$ , the interfacial energy, are used in place of the free energies, where  $w_A \approx 2\sqrt{\gamma_1\gamma_2}$ . Consequently, the determi-

nation of the Dupré surface energy requires values of the surface tension. Gilman (1960) has measured the surface energy for several materials and proposed an empirical model to calculate the surface energy:

$$\gamma = (E/y_0)(a_0/\pi)^2, \quad (8)$$

where  $y_0$  is the equilibrium lattice constant and  $a_0$  is the elastic range of the attractive force. A comprehensive table of the measured values of  $y_0$ ,  $a_0$ , and surface energy is given by Buckley (1981). According to Buckley,  $a_0$  for silicon is 1.17Å and  $y_0$  is a variable of the crystal plane, varying from about 2Å to 3Å. For stainless steel, no measurements are available. The values of  $a_0$  and  $y_0$  for stainless steel are estimated based on the measurements of other metals, such as Cu and Fe. The chosen value for  $a_0$  ranges from 1.0Å to 1.8Å and  $y_0$  ranges from 2Å to 3Å. Then, using the high and low values of the Young's modulus for both stainless steel and silicon as stated above, the range of the surface energy  $\gamma$  for stainless steel becomes from 0.64 N/m to 3.45 N/m and for silicon, from 0.60 N/m to 1.17 N/m. Thus, the Dupré surface energy ranges from 1.24 N/m to 4.02 N/m. Again assuming that this represents the  $\pm 3\sigma$  points of a Gaussian distribution, the mean and standard deviation of the surface energy are  $\mu_w = 2.63$  N/m and  $\sigma_w = 0.46$  N/m.

### The Microsphere Radius, $r$

The range of the microsphere radius is determined from the measurements taken by a phase Doppler particle analyzer of the microspheres used in previous experimental work. A histogram of the radius measurements is plotted in Figure 1. For the DOE study, the average radius is  $\mu_r = 33.0 \mu\text{m}$  and the standard deviation is  $\sigma_r = 8.0 \mu\text{m}$ .

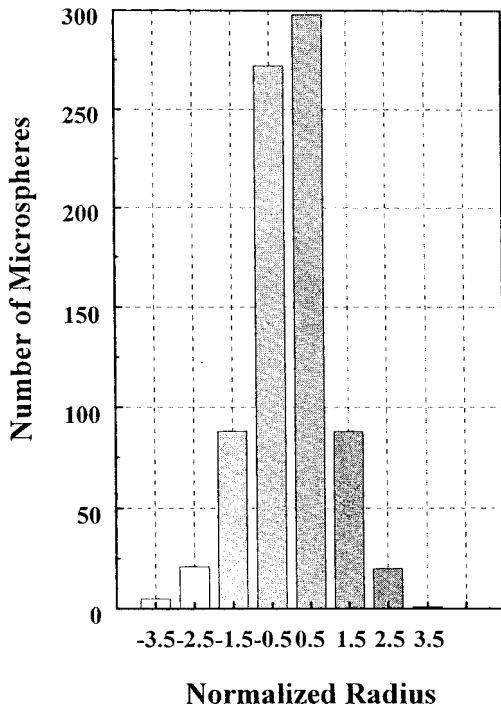


FIGURE 1. Sample distribution of stainless steel microspheres; radii are normalized to the distribution standard deviation.

*The Damping Coefficient,  $\zeta_A$  and  $\zeta_H$*

Two damping coefficients are used in the simulation model to represent energy dissipation. One,  $\zeta_A$ , is for adhesion damping and another,  $\zeta_H$ , for material (Hertzian) damping. These two coefficients are determined by matching experimental data at low and high initial normal velocities, re-

spectively. For a high initial velocity (when adhesion dissipation is negligible),  $\zeta_A$  is set to a value of zero and  $\zeta_H$  is chosen by matching the experimental measured coefficient of restitution. With that value of  $\zeta_H$ , a value of  $\zeta_A$  is then found by again matching the coefficient of restitution, but now at a low initial velocity. By iteratively repeating this process, a pair of nominal values of  $\zeta_A$  and  $\zeta_H$  is found that matches the coefficient of restitution over the desirable range of initial velocities. This process and results for materials analyzed here are described in Brach and Dunn (1998). Experimental error bounds for the coefficient of restitution have been estimated at the 95% level of confidence. These are used to determine corresponding 95% statistical distribution limits for the low and high values of coefficients  $\zeta_A$  and  $\zeta_H$ . These distributions give  $\mu_A = 630$ ,  $\sigma_A = 15$ ,  $\mu_H = 5$ , and  $\sigma_H = 2.5$ .

A summary of the results of the above estimations and the corresponding low and high values of the realistic factor variations is given in Table 1, along with the uniform variations based on  $\pm 5\%$  of the mean or nominal values.

*Approach to Determine the Capture Velocity,  $v_c$*

For each combination of factor values, coefficients of restitution are calculated for impacts over a range of initial normal velocities of 0 to 1.6 m/s. Then a curve fitting

TABLE 1. The two sets of low and high values of the 5 factors.

Factor	Realistic Variations		Uniform	
	Low/ High Value	%	Low/ High Value	%
A Hertzian stiffness, K	119.4/130.0, N/m <sup>2</sup>	$\pm 4.3\%$	118.5/130.9, N/m <sup>2</sup>	$\pm 5\%$
B Dupré surface energy, $w_A$	2.17/3.09, N/m	$\pm 17.5\%$	2.50/2.75, N/m	$\pm 5\%$
C microsphere radius, r	25.0/41.0, $\mu\text{m}$	$\pm 24.2\%$	31.35/34.65, $\mu\text{m}$	$\pm 5\%$
D damping coefficient, $\zeta_A$	615/645	$\pm 2.4\%$	598.5/661.5	$\pm 5\%$
E damping coefficient, $\zeta_H$	2.5/7.5	$\pm 50.0\%$	4.75/5.25	$\pm 5\%$

procedure is used to determine the capture velocity. The rigid body model relates the impact coefficients through the equation  $e = R(1 - \rho)$ . The corresponding equation with fitted constants  $\kappa_1$ ,  $\kappa_2$ , and  $v_c$  is given by Brach et al. (1998) as

$$e = R(1 - \rho) = \left( \frac{\kappa_1}{\kappa_1 + v_n} \right) \left( 1 - \frac{\kappa_2}{\kappa_2 + |v_n - v_c|} \right) \quad (9)$$

where  $\rho$  and  $e$  are highly dependent on the initial velocity,  $v_n$ . The constants  $v_c$ ,  $\kappa_1$ , and  $\kappa_2$  are determined using a nonlinear least-squares fitting procedure. A typical plot of the curve fitting is shown in Figure 2. Note from Equation 9 that when  $v_n = v_c$ ,  $\rho = 1$  and  $e = 0$ .

**CAPTURE VELOCITIES AND RESULTS OF THE SIMULATION**

Table 2 shows the factor level combinations and experimental layout for a  $2^{5-1}$  fractional factorial design where, in the exponent, 5 represents the number of factors and 1 is the factorial fraction. The (- / +) signs represent the corresponding (low/high) levels of each factor value from Table 1. Data collected according to such a factorial scheme allows the efficient calculation,

**TABLE 2. Fractional factorial layout.**

Factors					Response Values	
					Realistic	Uniform
A	B	C	D	E	$v_c$ m/s	$v_c$ m/s
-	-	-	-	+	0.145	0.139
+	-	-	-	-	0.150	0.127
-	+	-	-	-	0.262	0.154
+	+	-	-	+	0.250	0.143
-	-	+	-	-	0.077	0.122
+	-	+	-	+	0.073	0.119
-	+	+	-	+	0.177	0.138
+	+	+	-	-	0.166	0.126
-	-	-	+	-	0.158	0.144
+	-	-	+	+	0.148	0.135
-	+	-	+	+	0.271	0.174
+	+	-	+	-	0.251	0.159
-	-	+	+	+	0.081	0.127
+	-	+	+	-	0.075	0.116
-	+	+	+	-	0.138	0.149
+	+	+	+	+	0.180	0.135

or estimation, of how the factors and their interactions influence the response variable. For the design used here, main effects, ME, are calculated (Guttman et al. 1982) using the equation

$$ME = \frac{1}{2^3} \left[ \sum_{i=1}^{2^{5-1}} \pm v_{ci} \right] \quad (10)$$

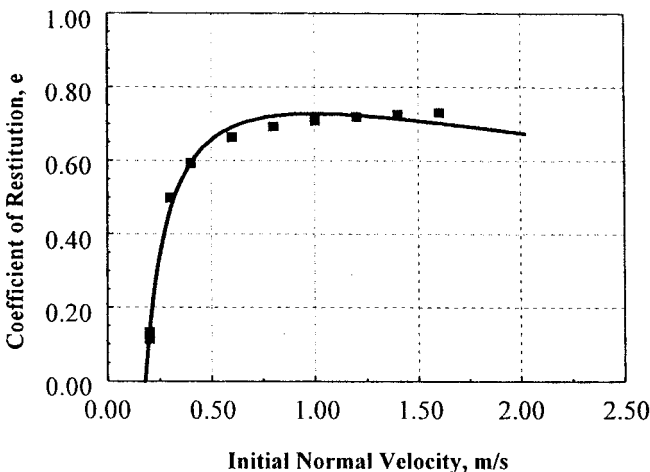


**FIGURE 2.** Experimental measurements, ■, of stainless steel microspheres and a silicon substrate fit to Equation 9. The capture velocity is 0.18 m/s.

The  $\pm$  signs in Equation 10 are those corresponding to the appropriate column in Table 2 for each single effect,  $A, B, \dots, E$  and the interactions. For example, the main effect of  $A$  for the case of realistic variations is  $ME_A = (-0.145 + 0.150 - 0.262 + \dots + 0.180)/8 = -0.002$  or  $-0.2\%$ . Because fractional factorial designs are used here, the main effects of the factors and the factor interactions are aliased or confounded. An inherent assumption is that the effects of the high order interactions (the interactions between combinations of 3 or more of the 5 factors) are negligible or insignificant. Furthermore, if the controlled variations of a number of factors produce no significant effects on the capture velocity, the main effect calculated from Equation 10 of those factors tend collectively to behave as a small random *error*. On the other hand, if a factor's variations significantly affect the capture velocity, its main effect will stand out from the others. Consequently, the significance of the individual factors and lower order interactions can be determined by plotting the main effects and interactions of the factors against normal probability coordinates. So the main effects, such as the  $-0.2\%$  for factor  $A$  (Hertzian stiffness) as calculated above, are plotted along the abscissa in Figures 3 and 4. The probability coordinates for the ordinate values are computed using a formula based on order statistics as described in Guttman et al. (1982). Those points that stand out, away from the random variations near a normal probability line, indicate significant factors. The relative distance from the line indicates the relative significance of the factor.

**DISCUSSION AND CONCLUSIONS**

When the factor effects from a fractional factorial are plotted on normal probability paper, they form a pattern. Those effects

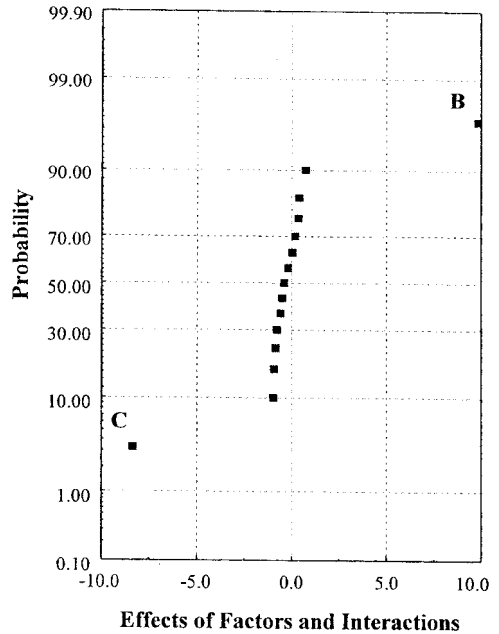


**FIGURE 3.** Values of the main effects for realistic variations.

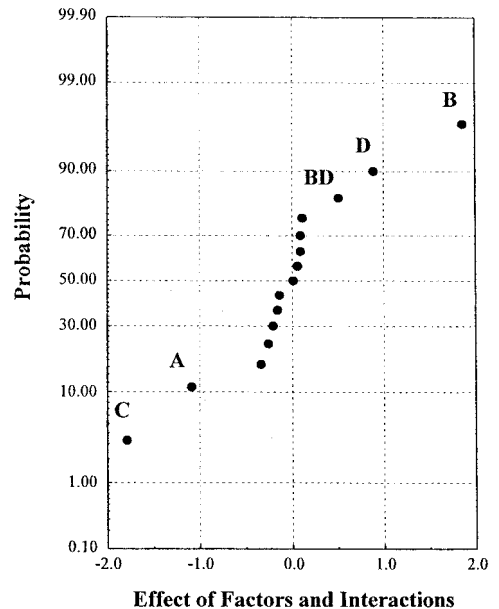


**FIGURE 4.** Values of the main effects for uniform variations.



that play a (relatively) insignificant role in influencing the response typically behave as “random error,” often with an approximately normal distribution (straight line). Factors to which the response variable is highly sensitive are not randomly distributed and stand out. A question that arises is why should the insignificant effects exhibit a normally distributed random behavior when calculations are from a theoretical simulation? There are at least two reasons. First of all, the extrapolation process (as described above) used to estimate  $v_c$  is not exact and introduces variations. Second, this is a fractional factorial design and so the insignificant effects, including high order interactions, are confounded and this confounding is likely to be irregular or random.

Figure 3 shows the main effects of the realistic variations and readily indicates that all but two of the effects are insignificant. The two are  $B$ , the Dupré surface energy, and  $C$ , the microsphere radius. In essence this means that the (- / +) levels of the radius and the Dupré energy had an overwhelming influence on the capture velocity compared to the changes of the other 3 factors, and to all interactions. For example, the change in Hertzian stiffness from 119.4 to 130.0 has little or no effect in influencing the capture velocity compared to the change of 25  $\mu\text{m}$  to 41  $\mu\text{m}$  in the radius. It is rather clear that  $w_A$  and  $r$  are not only the most significant factors in influencing the capture velocity but also that they totally outweigh the others. Note also that the signs of the effects indicate the “direction” of influence. The main effect due to the radius,  $C$ , is negative, so the capture velocity is inversely related to radius. The sign of the surface energy factor,  $B$ , is positive, so the greater the energy, the more likely capture will occur.

Figure 4 shows that for uniform percentage variations, other factors assume signif-

icance. Factors  $B$  (Dupré surface energy) and  $C$  (microsphere radius) remain dominant, but  $A$  (Hertzian stiffness) and  $D$  (adhesion damping) now show significance. In addition, the second order interaction,  $BD$ , of the Dupré surface energy and adhesion damping displays significance.

Fractional factorial designs are known for their efficiency, but they have a disadvantage in that the effects of the factors are tied up, or confounded, with higher order interactions. The results displayed in Figures 3 and 4 clearly show that all third- and fourth-order interactions (as well as all but one second-order interaction) are insignificant. Consequently, it can be concluded safely that for the ranges of variations of the factors used in the study, capture is controlled overwhelmingly by the particle size and the Dupré surface energy. Other factors such as the Hertzian stiffness and the adhesion damping will be significant, particularly if the radius and Dupré energy remain relatively constant, but interactions can be disregarded.

---

*The research described in this article was supported in part by the Center for Indoor Air Research (Contract No. 96-06) and in part by the Electric Power Research Institute (Contract No. RP 8034-03).*

---

## NOMENCLATURE

- $a$  Hertzian contact radius, m;
- $a_0$  range of attractive force, m;
- $d$  microsphere diameter, m;
- $E$  modulus of elasticity, Pa;
- $e$  overall, kinematic coefficient of restitution;
- $F$  specific surface free energy,  $\text{J}/\text{m}^2$ ;
- $f_0$  magnitude of (van der Waals) adhesion ring force,  $\text{N}/\text{m}$ ;
- $K$  Hertzian elastic constant,  $\text{N}/\text{m}^2$ ;
- $k_i$  elastic constant (sphere and surface),  $\text{m}^2/\text{N}$ ;

- $m$  mass of the sphere, kg;  
 $n$  normal displacement of the mass center, m;  
 $r$  Hertzian radius, m;  
 $R$  kinematic coefficient of restitution in the absence of adhesion;  
 $v_c$  capture velocity, m/s;  
 $v_n$  initial normal velocity, m/s;  
 $w_A$  Dupré surface energy\*, J/m<sup>2</sup>;  
 $y_0$  equilibrium lattice constant, m;  
 $\gamma$  surface energy\*, J/m<sup>2</sup>;  
 $\kappa$  constant in an empirical equation, m/s;  
 $\mu$  mean of a statistical distribution;  
 $\sigma$  standard deviation of a statistical distribution;  
 $\rho$  adhesion impact coefficient;  
 $\nu_i$  Poisson's ratio (sphere and barrier);  
 $\zeta_A$  nondimensional adhesion dissipation constant;  
 $\zeta_H$  nondimensional material dissipation constant.

## References

- Brach, R. M., and Dunn, P. F. (1995). Macro-dynamics of Microparticles, *Aerosol Sci & Tech* 23:51–71.
- Brach, R. M., and Dunn, P. F. (1998). Models of Rebound and Capture for Oblique Microparticle Impacts, *Aerosol Sci & Tech* 29:379–388.
- Brach, R. M., Dunn, P. F., and Li, X. (1998). *Modeling of Microparticle Transition from Rebound to Capture*, Proceedings of the 21st Annual Meeting of the Adhesion Society, Savannah, GA, pp. 271–273.
- Buckeley, D. H. (1981). *Surface Effects in Adhesion, Friction, Wear, and Lubrication*, Elsevier Scientific Publishing Company, New York.
- Derjaguin, B. V., Muller, V. M., and Toporov, Y. P. (1975). Effect of Contact Deformations on the Adhesion of Particles, *J. Colloid Interface & Sci* 53:314–326.
- Dunn, P. F., Brach, R. M., and Caylor, M. J. (1995). Experiments on the Low Velocity Impact of Microspheres with Planar Surfaces, *Aerosol Sci & Tech* 23:80–95.
- Gere, J. M., and Timoshenko, S. P. (1990). *Mechanics of Materials*, PWS-Kent Publishing Co, Boston, MA.
- Gilman, J. J. (1960). Direct Measurement of the Surface Energies of Crystals, *J. of Appl Physics* 31:2208–2218.
- Guttman, I., Wilks, S., and Hunter, J. (1982). *Introductory Engineering Statistics*, 3rd Ed., John Wiley & Sons, New York.
- Horn, R. G., Israelachvili, J. N., and Pribac, F. (1987). Measurement of the Deformation and Adhesion of Solids in Contact, *J. of Colloid and Interface Sci* 115:492.
- Israelachvili, J. N. (1985). *Intermolecular and Surface Forces*, Academic Press, New York.
- Johnson, K. L., Kendall, K., and Roberts, A. D. (1971). *Proc. Royal Soc* 324:301–313.
- Johnson, K. L., and Pollock, H. M. (1994). The Role of Adhesion in the Impact of Elastic Spheres, *J. Adhesion Sci & Tech* 8:1323–1332.
- Lee, L. H. (1991). The Chemistry and Physics of Solid Adhesion. In *Fundamentals of Adhesion*, edited by L. H. Lee. Plenum Press, New York.
- Li, X., Dunn, P. F., and Brach, R. M. (1999). Experimental and Numerical Studies on the Normal Impact of Microspheres with Surfaces, *J. Aerosol Sci* 30:439–449.
- Wall, S., John, W., Wang, H.-C., and Goren, S. (1990). Measurement of Kinetic Energy Loss for Particles Impacting Surfaces, *Aerosol Sci & Tech* 12:926–946.
- Wortman, J. J., and Evans, R. A. (1965). Young's Modulus, Shear Modulus, and Poisson's Ratio in Silicon and Germanium, *J. of Applied Physics* 36:153–156.

\*Following common usage this is called surface energy in this paper, although it actually is energy per unit area.